J Solution Chem (2010) 39: 197–218
DOI 10.1007/s10953-010-9495-z

Solubility of B-Nb_2O_5 and the Hydrolysis of Niobium(V) in Aqueous Solution as a Function of Temperature and Ionic Strength

C. Peiffert · C. Nguyen-Trung · D.A. Palmer · J.P. Laval · E. Giffaut

Received: 23 April 2009 / Accepted: 30 July 2009 / Published online: 2 March 2010

Abstract B-Nb_2O_5 was recrystallized from commercially available oxide, and XRD analyses indicated that it is stable in contact with solutions over the pH range 0 to 9, whereas solid polyniobates such as $Na_8Nb_6O_{19}\cdot 13H_2O$(s) appear to predominate at pH > 9. Solubilities of the crystalline B-Nb_2O_5 were determined in five $NaClO_4$ solutions ($0.1 \leq I_m/\text{mol}\cdot\text{kg}^{-1} \leq 1.0$) over a wide pH range at (25.0 ± 0.1) °C and at 0.1 MPa. A limited number of measurements were also made at $I_m = 6.0$ mol·kg^{-1}, whereas at $I_m = 1.0$ mol·kg^{-1} the full range of pH was also covered at (10, 50 and 70) °C. The pH of these solutions was fixed using either $HClO_4$ (pH ≤ 4) or NaOH (pH ≥ 10) and determined by mass balance, whereas the pH on the molality scale was measured in buffer mixtures of acetic acid + acetate (4 ≤ pH ≤ 6), Bis-Tris (pH ≈ 7), Tris (pH ≈ 8) and boric acid + borate (pH ≈ 9). Treatment of the solubility results indicated the presence of four species, $Nb(OH)_n^{5-n}$ (where $n = 4$–7), so that the molal solubility quotients were determined according to:

$$0.5Nb_2O_5(\text{cr}) + 0.5(2n-5)H_2O(\text{l}) \rightleftarrows Nb(OH)_n^{5-n} + (n-5)H^+ \quad (n = 4\text{–}7)$$

and were fitted empirically as a function of ionic strength and temperature, including the appropriate Debye-Hückel term. A Specific Interaction Theory (SIT) approach was also attempted. The former approach yielded the following values of $\log_{10} K_{sn}$ (infinite dilution) at 25 °C: $-(7.4 \pm 0.2)$ for $n = 4$; $-(9.1 \pm 0.1)$ for $n = 5$; $-(14.1 \pm 0.3)$ for $n = 6$; and $-(23.9 \pm 0.6)$ for $n = 7$. Given the experimental uncertainties (2σ), it is interesting to note

C. Peiffert · C. Nguyen-Trung
UMR 7566 G2R, Nancy Université, CNRS, CREGU, BP 239, 54506 Vandœuvre-lès-Nancy Cédex, France

D.A. Palmer (✉)
CASD (retired), ORNL, Bldg 4500S, Oak Ridge, TN 37831-6110, USA
e-mail: solution_Chemistry@comcast.net

J.P. Laval
Fac. Sciences, SPCTS, UMR CNRS 6638, 123 Ave. A. Thomas, 87060 Limoges Cédex, France

E. Giffaut
ANDRA, Parc de la Croix Blanche, 1-7 rue J. Monnet, 92298 Chatenay-Malabry Cédex, France

that the effect of ionic strength only exceeded the combined uncertainties significantly in the case of $\log_{10} K_{s6}$ to $I_m = 1.0$ mol·kg^{-1}, such that these values may be of use by defining their magnitudes in other media. Values of $\Delta_f G^o$, $\Delta_f H^o$, S^o and C_p^o (298.15 K, 0.1 MPa) for each hydrolysis product were calculated and tabulated.

Keywords Solubility · Niobium(V) · Aqueous solution · Thermodynamics · Speciation · SIT

1 Introduction

Niobium and tantalum exhibit comparable chemical properties largely because of their identical ionic radii (Nb^{5+}, Ta^{5+}: 64 pm) and their common occurrence in the same oxidation states [1]. Niobium and tantalum are utilized in microelectronics, the fabrication of semiconductor components, and the production of various types of catalysts and materials with special electro-physical characteristics. In geochemistry, they are useful natural tracers to elucidate the evolution of Earth's major crustal and mantle reservoirs [2]. Both elements display very low mobility except in the most extreme environments, tantalum oxide being the less soluble of the two. The presence of citric, tartaric and oxalic acids enhances their solubility through chelation.

Anthropogenic sources of niobium include nuclear fuel production, welding and steel production [3], and it can also be present as a fission product in significant quantities, mainly as oxides [4]. Moreover, neutron-activated wastes contain significant amounts of long-lived, non-transuranic radioactive isotopes such as ^{94}Nb (with a half-life of 2.0×10^4 years) in the pressure vessel and its internal components. The thermodynamic properties of aqueous niobium species are therefore fundamental in modeling niobium release from nuclear waste stored in deep underground vaults in contact with natural hydrothermal systems. However, despite the practical importance of niobium and tantalum whereby their mineralogy and geochemistry have been investigated in great detail, little is still known about the hydrolysis behavior of their dissolved species, especially at low concentrations.

Consequently, controversy exists as to the speciation of Nb(V) species in solution at low concentrations [5, 6], although the stabilities of the polynuclear Nb(V) species at concentrations traditionally accessible to conventional techniques such as potentiometry and spectrophotometry appear to be well established [6–15]. Solubility measurements have long provided a means of investigating solution speciation at the low concentrations generally imposed by a solid oxide/hydroxide phase [16]. However, in the case of Nb(V), concern has been raised as to the presence of colloidal material which would greatly enhance the solubility of the mother phase, and to changes in the morphology of the solid as a function of pH.

The solubility of freshly precipitated, active Nb_2O_5 has been measured at 19 °C over the pH ranges −0.78 to 0.0 (HNO_3) and 7.00 to 9.73 (1 mol·dm^{-3} KNO_3) [5]. The solid phase was not characterized but was assumed to be amorphous. These authors reported a solubility minimum corresponding to the formation of $Nb(OH)_5^0$ at a concentration of 1.6×10^{-5} mol·dm^{-3}, or $\log_{10} Q_{s5} \approx -4.8$ for this material, that is sufficiently high as to virtually assure that it was indeed amorphous. From these somewhat dubious results, two step-wise hydrolysis equilibria were proposed:

$$Nb(OH)_4^+ + H_2O(l) \rightleftarrows Nb(OH)_5^0 + H^+ \quad (1)$$

$$Nb(OH)_5^0 + H_2O(l) \rightleftarrows Nb(OH)_6^- + H^+ \quad (2)$$

yielding $\log_{10} Q_{45} \approx 0.6$ and $\log_{10} Q_{56} \approx -7.8$. If no change in the nature of the solid phase had occurred during these measurements, these hydrolysis constants could in principle be of value, although in the absence of any solid phase information and because of the scant data reported (with no mention of how the pH was fixed or measured), these constants are only provisional at best. Indeed, the current study estimates markedly different values of the constants at 20 °C of −2.1 and −6.1, respectively, admittedly in 1 mol·kg^{-1} ($NaClO_4$).

The remaining studies of Nb(V) hydrolysis were confined to higher concentrations, i.e., $\geq 10^{-3}$ mol·dm^{-3}, where the polynuclear Nb(V) species predominate and the results are quite unambiguous. Three hydrolysis equilibria have been reported from potentiometric and spectrophotometric studies [7–15], namely:

$$Nb_6O_{16}(OH)_3^{5-} \rightleftarrows Nb_6O_{19}^{8-} + 3H^+ \tag{3}$$

$$Nb_6O_{17}(OH)_2^{6-} \rightleftarrows Nb_6O_{19}^{8-} + 2H^+ \tag{4}$$

$$Nb_6O_{18}(OH)^{7-} \rightleftarrows Nb_6O_{19}^{8-} + H^+ \tag{5}$$

Etxebarria et al. [7], in a careful potentiometric study of these equilibria mainly at $I_m = 3.44$ (3 mol·dm^{-3} KNO_3, converted here to molal units), reported the following hydrolysis constants at (25.0 ± 0.1) °C: $\log_{10}\beta$ (Eq. 3) = −(32.72 ± 0.07); $\log_{10}\beta$ (Eq. 4) = −(23.43 ± 0.04); $\log_{10}\beta$ (Eq. 5) = −(13.57 ± 0.04), which are, in general, in reasonable agreement with earlier results at this experimental condition [9, 13]. They also determined the ionic strength dependence of these hydrolysis constants using Bromley's extended Debye-Hückel approach that, in view of the extremely high anionic charges involved, is suspect if taken further than providing a purely empirical functional fit. Finally, Etxebarria and coworkers attempted to rationalize the solubility data of Babko et al. [5] to define the stability boundary between $Nb(OH)_5^0$ and $Nb_6O_{16}(OH)_3^{5-}$. The uncertainty of this calculation appears to have been grossly underestimated, due to the experimental uncertainties in the latter work, but it is relevant to mention that they predict that monomers will dominate below $m_{Nb} = 10^{-5}$ at pH < 7.5, decreasing to almost 10^{-6} at pH ≈ 9. Obviously, m_{Nb} will be raised to the sixth power and, if one were to consider the formation equilibria of these polynuclear species with respect to the monomeric Nb(V) species such that at 10^{-5} mol·kg^{-1} (which represents about the maximum concentration at $pH_m < 9$ reached in the current study) the stabilities of the polynuclear anions that were investigated previously at $> 10^{-3}$ mol·kg^{-1} would decrease by a factor of 10^{12}. Note that without knowledge of the polymerization constants, predominance diagrams, which would otherwise more clearly illustrate this point, cannot be created.

Guillaumont et al. [17] reported an extensive series of solvent extraction measurements performed at 25 °C on niobium(V) solutions over a wide range of pH (1–9) in 0.1 and 3.0 mol·dm^{-3} ($LiClO_4$). However, the results are only presented in the form of figures. They recorded only one hydrolysis constant with $\log_{10} K_{45} = -3.2$ ($I_m = 0.101$ mol·kg^{-1}), which is in poor agreement with that derived in the present study of −(1.7 ± 0.2) at $I_m = 0.101$ mol·kg^{-1} ($NaClO_4$). No explanation for this disparity can be offered at this time.

Finally, it is of interest to note that in 1953, Lindqvist [18] had already established from X-ray powder measurements the existence of a $Nb_6O_{19}^{8-}$ unit cell in the phase $7Na_2O{\cdot}6Nb_2O_5{\cdot}32H_2O$, lending even more credence to the presence of Nb hexameric species in solution at millimolar and higher concentrations of niobium(V).

2 Experimental

2.1 Solid Phase

Crystalline B-Nb_2O_5 was prepared by heating Aldrich reagent grade Nb_2O_5 (reported purity = 99.99%) up to 1000 °C at 0.1 MPa for ten hours. X-ray powder diffraction analysis indicated the presence of pure B-Nb_2O_5 within our ability to resolve the principal peaks that are listed in Table 1. B-Nb_2O_5 is referred to in some sources as the high-temperature phase, e.g. [19]. More than 95% of the Nb_2O_5 crystals had grain sizes in the range 5 to 10 μm as shown by SEM analysis (Fig. 1). Earlier concerns mentioned by Etxebarria et al. [7], that in the past Nb_2O_5 solubility measurements were hampered by colloid formation and to variations in solid-phase composition and/or structure, were not evident in our study.

TGA was used to determine the water content of the pristine recrystallized B-Nb_2O_5 as well as to track possible hydration and/or phase alteration of the solid, particularly as a function of pH. Figure 2 shows three thermogravimetric traces (temperature in Celsius on the LHS ordinate, percent weight loss on the RHS versus time on the abscissa). The unreacted and acid-equilibrated samples (Nb1 and Nb3, respectively) showed $< 0.025\%$ mass loss by 200 °C (loss of one mole of water of crystallization would correspond to 6.77%), clearly demonstrating that the solid phase remained anhydrous under these conditions; even by 800 °C the weight loss was only ca. 0.125%. The solid reacted with dilute NaOH, on the other hand, showed a continuous weight loss that implies some initial dehydration followed by a probable phase change to reconstitute the oxide with a 0.66% total weight loss. As discussed below, this behavior supports the conclusion that in acidic and near-neutral pH solutions the solid phase remains unaffected (i.e., crystalline B-Nb_2O_5 predominates), whereas at moderately high pH a hydroxylated multinuclear niobium(V) phase may be formed at least on the surface of the oxide particles, noting that an XRD analysis of the latter material failed to show the presence of crystalline sodium niobate.

2.2 Solutions

The aqueous solutions used in this study were prepared on a mass basis by dilution of the following stock solutions with deionized water (resistivity: 18.2 MΩ·cm) to concentrations of 0.01, 0.05 and 0.1 mol·kg^{-1}. Solutions of 1–6 mol·kg^{-1} $NaClO_4$ were prepared from Merck reagent grade $NaClO_4$ and were standardized by pH titration of the leachate from a Dowex cation exchange resin column in the hydrogen ion form. A 1 mol·kg^{-1} $HClO_4$ solution (prepared from Aldrich, reagent grade 70%) was standardized by pH titration against a solution of oven-dried Na_2CO_3. A 1 mol·kg^{-1} NaOH (Aldrich, reagent grade) solution was prepared by diluting 50 wt-% NaOH and then was standardized by pH titration against the stock $HClO_4$ solution. A 1 mol·kg^{-1} CH_3CO_2H (Aldrich, glacial grade 99.8%) solution was prepared by mass and standardized by pH titration against the stock $HClO_4$ solution, and 1 mol·kg^{-1} solutions of $(HOCH_2)_3CN(HOCH_2CH_2)_2$ or Bis-Tris (Aldrich, reagent grade, 99+%), $(HOCH_2)_3CNH_2$ or Tris (Aldrich, reagent grade, 99.8%), and $B(OH)_3$ (Aldrich, reagent grade) were prepared by mass. All stock solutions were stored in 50 cm^3 disposable polyethylene/polypropylene syringes (Aldrich Chemical Co.). The starting solution compositions were known to better than 0.1% and also served as standard solutions for the calibration of the $pH_m (\equiv -\log_{10} m_{H^+})$ measurements, as discussed below.

2.3 Experimental Procedure

The experiments were conducted in 50 cm^3 polypropylene/polyethylene syringes mounted on a rotating cylindrical sample holder that was completely submerged in a 200 L water

Table 1 Comparison of the main peak positions in the XRD patterns of Nb_2O_5(cr)

Lit.[a] d (Å)	Intensity	Our study d (Å)	Lit.[a] d (Å)	Intensity	Our study d (Å)
10.575	8	10.568	2.316	19	2.316
9.669	2	9.673	2.211	1	2.211
9.192	4	9.183	2.165	2	2.165
8.399	3	8.401	2.113	3	2.113
6.304	5	6.302	2.078	19	2.078
5.595	2	5.601	2.038	18	2.038
5.284	5	5.284	1.993	2	1.995
5.122	23	5.124	1.924	3	1.925
4.743	3	4.740	1.912	35	1.915
4.728	4	4.731	1.871	3	1.872
4.625	18	4.625	1.820	12	1.821
3.866	3	3.866	1.790	8	1.789
3.828	6	3.825	1.767	4	1.767
3.745	83	3.744	1.757	3	1.757
3.642	100	3.642	1.743	12	1.743
3.557	9	3.557	1.728	8	1.728
3.523	19	3.523	1.710	6	1.710
3.489	79	3.490	1.693	20	1.693
3.383	7	3.383	1.689	16	1.689
3.355	23	3.354	1.684	28	1.684
3.160	7	3.159	1.680	20	1.680
3.089	2	3.087	1.677	17	1.677
3.000	4	3.000	1.656	3	1.656
2.864	6	2.863	1.628	7	1.628
2.835	35	2.835	1.593	15	1.593
2.828	31	2.828	1.583	16	1.582
2.775	23	2.775	1.580	15	1.580
2.707	24	2.706	1.557	17	1.557
2.699	13	2.698	1.529	9	1.530
2.633	3	2.633	1.517	5	1.518
2.546	20	2.545	1.502	4	1.502
2.493	13	2.493	1.455	6	1.456

[a]Nb_2O_5; monoclinic; S.G.: P2; $a_{ref} = 20.38100$ Å ($a_{exp} = 20.3819$ Å), $b_{ref} = 3.82490$ Å ($b_{exp} = 3.82475$ Å), $c_{ref} = 19.36800$ Å ($c_{exp} = 19.3660$ Å), $\beta_{ref} = 115.694°$ ($\beta_{exp} = 115.698°$); radiation: Cu Kα_1; $L = 1.540596$ Å; reference pattern: 00-037-1468; CAS number: 1313-96-8. See McMurdie, H., Morris, M., Evans, E., Paretzkin, B., Wong-Ng, W., Zhang, Y.: Standard X-ray diffraction powder patterns from the JCPDS Research Associateship. Powder Diffr. **1**, p. 342 (1986). In parentheses, our experimental, refined lattice parameter values

bath that controlled the temperature of the syringes to better than ±0.05 °C. Temperature gradients within the bath were found to be less than ±0.02 °C. The syringes were positioned on the cylinder such that they rotated lengthwise at a rate of one revolution per minute. Under

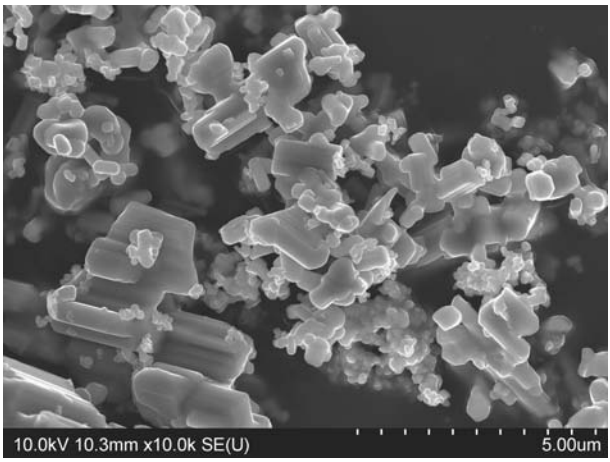

Fig. 1 An SEM image of the recrystallized B-Nb_2O_5

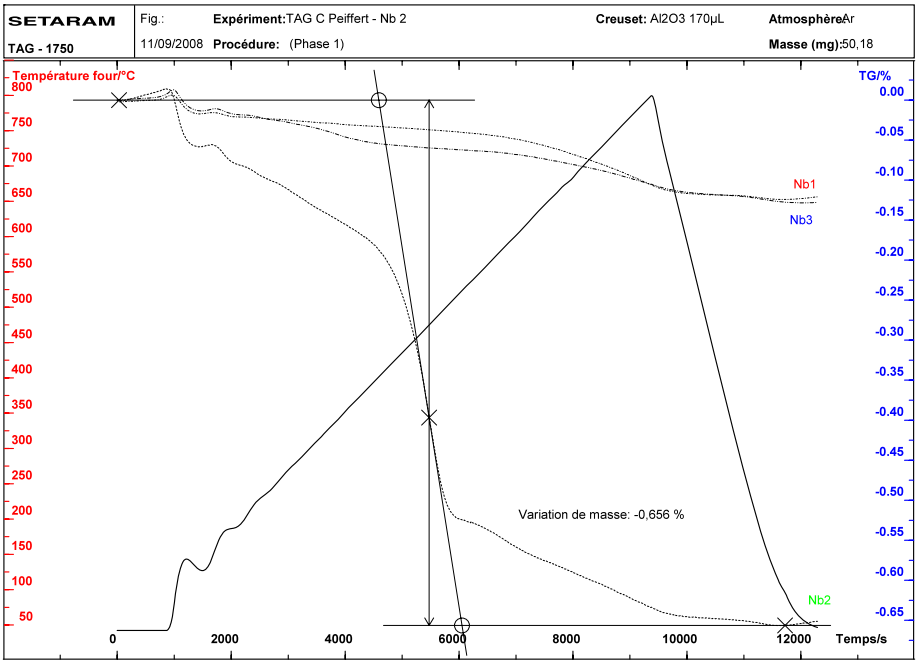

Fig. 2 A TGA of recrystallized B-Nb_2O_5 (Nb1: *dot-dashed curve*); recovered solid after exposure to 10^{-3} mol·kg^{-1} HCl for 35 days (Nb3; *dot-dot-dashed curve*); (**b**) recovered solid after exposure to 10^{-3} mol·kg^{-1} NaOH for 35 days (Nb2; *short-dashed curve*)

these conditions, the solid charge was in constant motion without physical degradation of the B-Nb_2O_5 crystals. Each syringe contained approximately 1 g of B-Nb_2O_5 and 50 cm^3 of starting solution.

Samples were taken after 5, 10, 15 and 30 days. At each sampling, a syringe containing the suspension was removed, dried, and approximately 13 cm^3 of solution were transferred to a second syringe via a Millipore Swinnex disc filter holder (13 mm diameter) fitted with

a Millipore PTGC (10^4 Nominal Molecular Weight Limit) ultrafiltration disc membrane. About 10 cm^3 of the sample were transferred to a 20 cm^3 beaker for niobium analysis. For acidic (pH $\leq$ 4) solutions, equilibrium (i.e., constant niobium concentration) was attained after 15 days. In the pH range 4 to 9, a minimum of 30 days was necessary to reach equilibrium. The ionic strength, I_m, in the range 0.1–6.0 mol·kg^{-1} seemed to have no effect on the kinetics of dissolution of niobium oxide.

The pH of solutions containing either $HClO_4$ or NaOH was estimated from the stoichiometric molalities, making use in the latter case of the acid-dissociation quotient of water with allowance for the contributions of Nb(V) species to the ionic strength based on the cited SIT parameters in a $NaClO_4$ medium, giving $pK_w = 14.001$ at 25 °C [20]. The pHs of the equilibrated samples containing pH buffers were measured using a Ross combination glass electrode, coupled to an Orion 520 pH-meter. Approximately 3 cm^3 aliquots of the filtered sample were transferred to a 5 cm^3 beaker containing a micro magnet that was then sealed on the electrode with a rubber stopper. The assembly was then placed in a thermostatted bath (Heto Laboratory Equipment) at 10.0, 25.0, 50.0 and 70.0 (±0.1) °C and stirred magnetically. The pH meter was calibrated at temperature against standard solutions consisting of the original $NaClO_4$ stock solutions used to equilibrate with the B-Nb_2O_5 solid, where the pH is defined on the hydrogen ion molality scale throughout the present study and is therefore represented here as pH_m[8]. The final pH_m value of the sample was obtained after correction for the liquid-junction potential between the aqueous sample and the standard solution, which were at the same ionic strength, using the Henderson equation [6] with the limiting equivalent conductivity values of the ions H^+, Na^+ and ClO_4^- taken from Robinson and Stokes [21]. The calculated liquid-junction potentials varied in the range 0.1–1.3 mV, with the maximum value of 1.3 mV, corresponding to 0.02 pH_m units with an estimated uncertainty of ±10%. The overall experimental uncertainty in the pH_m measurements was estimated to be ±(0.1 to 0.2). For the stoichiometric pH_m standard values, the estimated uncertainty was < 0.02.

2.4 Analytical Method

The niobium concentration in each aqueous sample was determined using the inductively coupled plasma mass spectrometric (ICP-MS) technique. The detection limit of this technique was 10^{-10} mol·kg^{-1} with an experimental uncertainty of ±10%.

3 Results and Discussion

Table 2 gives the logarithms of the total niobium molality, $\log_{10} m_{Nb}$, at each value of pH_m for the experiments conducted at 25.0 °C (0.1 MPa) for the five ionic strengths studied (I_m = 0.1, 0.3, 0.5, 1.0 and 6.0 mol·kg^{-1} $NaClO_4$). The corresponding values measured in I_m = 1.0 mol·kg^{-1} ($NaClO_4$) solutions at 10, 50 and 70 °C are listed in Table 3.

The solubility, $\log_{10} m_{Nb}$, profiles in the pH_m range ≈ 1 to 9 are illustrated in Figs. 3a–e and 4a–c, based on the results listed in Tables 2 and 3, respectively. The upper pH_m limit was imposed by the observed change in the morphology of the solid phase beyond this pH_m as will be discussed below. However, within the pH_m range of these plots, B-Nb_2O_5 was the only solid phase detected in the XRD powder patterns of the recovered solids (detection limit of XRD spectra is estimated at ±0.5%). The analysis of these solubility data sets was carried out using the ORNL ORGLS nonlinear least-squares fit program [6]. The major criterion for acceptance of a given fit was obtained from the goodness of fit factor, viz.:

Table 2 Molal-based solubilities of B-Nb_2O_5 as functions of pH_m and ionic strength at 25.0 °C

I_m	pH_m[a]	$-\log_{10} m_{Nb}$[b]	I_m	pH_m	$-\log_{10} m_{Nb}$
0.1	2.02	8.99	0.5	1.25	8.76
0.1	2.51	9.16	0.5	1.50	8.92
0.1	3.04	9.22	0.5	2.00	9.09
0.1	4.07	9.12	0.5	2.54	9.42
0.1	5.10	8.63	0.5	3.10	9.46
0.1	5.97	8.08	0.5	4.03	9.46
0.1	7.01	7.25	0.5	5.07	9.28
0.1	7.97	6.11	0.5	5.87	9.18
0.1	8.99	5.01	0.5	7.03	7.62
0.1	9.98	4.71	0.5	8.01	6.64
0.1	11.08	4.52	0.5	9.07	5.47
0.1	11.46	4.49	0.5	10.11	4.65
0.1	11.96	3.89	0.5	11.03	4.63
0.3	1.60	8.95	0.5	11.52	4.47
0.3	1.74	9.00	0.5	12.12	4.44
0.3	2.01	9.03	0.5	12.45	3.86
0.3	2.43	9.09	1.00	1.02	8.47
0.3	3.11	9.20	1.00	1.25	8.74
0.3	3.89	9.24	1.00	1.53	9.05
0.3	4.91	9.04	1.00	1.73	9.14
0.3	6.04	8.26	1.00	2.02	9.18
0.3	6.94	7.64	1.00	2.50	9.37
0.3	8.09	6.02	1.00	3.06	9.49
0.3	9.04	5.02	1.00	3.45	9.50
0.3	10.00	4.57	1.00	4.11	9.81
0.3	10.98	4.46	1.00	5.20	9.47
0.3	11.52	4.49	1.00	5.87	9.36
0.3	12.05	3.97	1.00	6.89	8.61
0.3	12.49	3.88	1.00	8.03	6.98
			1.00	9.08	6.08
			1.00	10.15	5.08
			1.00	11.07	4.62
			1.00	11.46	4.50
			1.00	12.00	4.41
			1.00	12.48	3.87
			1.00	13.00	3.60
			6.00	0.50	8.56
			6.00	1.00	8.96
			6.00	1.50	9.10
			6.00	2.00	9.26

[a]Experimental uncertainties for pH_m in the range $4 \leq pH_m \geq 10$ are ±0.02 with those in the intermediate range being 0.15

[b]Experimental uncertainties in $\log_{10} m_{Nb}$ are generally ±0.05

Table 3 Molal-based solubilities of B-Nb_2O_5 and pH_m values obtained at ionic strengths I_m = 1.0 mol·kg^{-1} as a function of temperature

t/°C	pH_m^a	$-\log_{10} m_{Nb}^b$	t/°C	pH_m	$-\log_{10} m_{Nb}$
10.0	0.99	8.35	50.0	3.02	9.37
10.0	1.32	8.57	50.0	3.51	9.37
10.0	1.59	9.01	50.0	4.02	9.49
10.0	1.67	9.12	50.0	4.98	9.19
10.0	1.97	9.27	50.0	5.97	8.97
10.0	2.11	9.27	50.0	7.03	8.39
10.0	2.53	9.49	50.0	8.02	6.37
10.0	3.01	9.67	50.0	9.05	4.93
10.0	3.51	9.65	50.0	10.00	4.06
10.0	3.99	9.67	50.0	11.03	3.78
10.0	5.02	9.59	50.0	11.11	3.09
10.0	6.01	9.48	50.0	11.52	2.91
10.0	6.98	9.18	50.0	11.56	3.65
10.0	7.99	7.75	50.0	12.06	3.43
10.0	9.03	6.60	50.0	12.48	2.89
10.0	10.01	5.90	50.0	13.04	2.79
10.0	11.06	5.24	70.0	1.00	7.50
10.0	11.46	5.26	70.0	1.24	8.10
10.0	12.03	5.13	70.0	1.51	8.40
10.0	12.48	4.67	70.0	1.75	8.70
10.0	12.89	4.34	70.0	2.02	9.06
50.0	1.10	8.35	70.0	2.52	9.30
50.0	1.30	8.59	70.0	3.00	9.31
50.0	1.50	8.89	70.0	3.51	9.30
50.0	1.78	9.07	70.0	3.98	9.30
50.0	2.01	9.12	70.0	4.99	8.99
50.0	2.49	9.27	70.0	6.05	8.80
			70.0	7.06	7.91
			70.0	8.05	6.40
			70.0	9.05	4.99
			70.0	10.03	3.40
			70.0	12.06	2.80
			70.0	12.49	2.40
			70.0	13.02	2.36

[a,b]The same as in Table 2

$$\text{Fit factor} = \sqrt{\frac{\sum w\{m_{Nb}(\text{obs}) - m_{Nb}(\text{calc})\}^2}{(n_O - n_V)}} \tag{6}$$

where m_{Nb}(obs) and m_{Nb}(calc) are the measured and calculated niobium molalities, respectively, w is the weighting factor, n_O is the number of observations and n_V is the number of variables or solubility constants. The weighting factor was assessed from the estimated experimental uncertainties in m_{Nb}(obs) and pH_m. These weighted fits indicated the possible

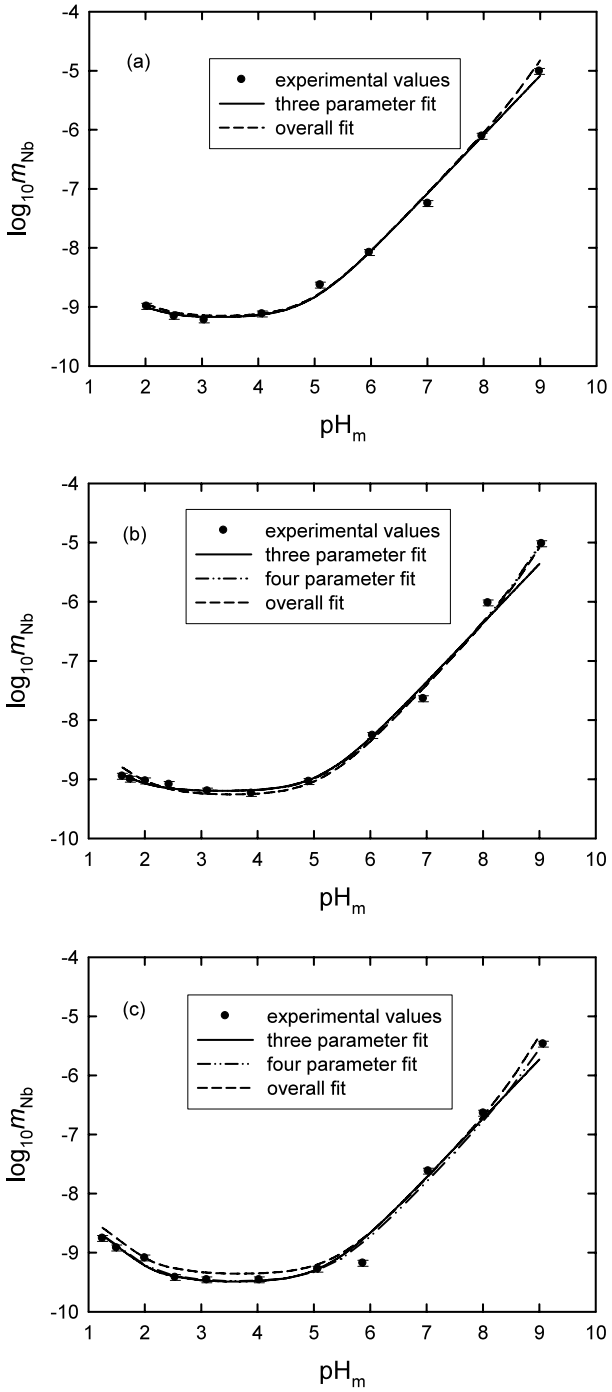

Fig. 3 Logarithm of the niobium(V) molality, $\log_{10} m_{\mathrm{Nb}}$, as a function of pH_m at 25 °C for various ionic strengths: 0.1 (**a**), 0.3 (**b**), 0.5 (**c**), 1.0 (**d**), and 6.0 (**e**) mol·kg^{-1}

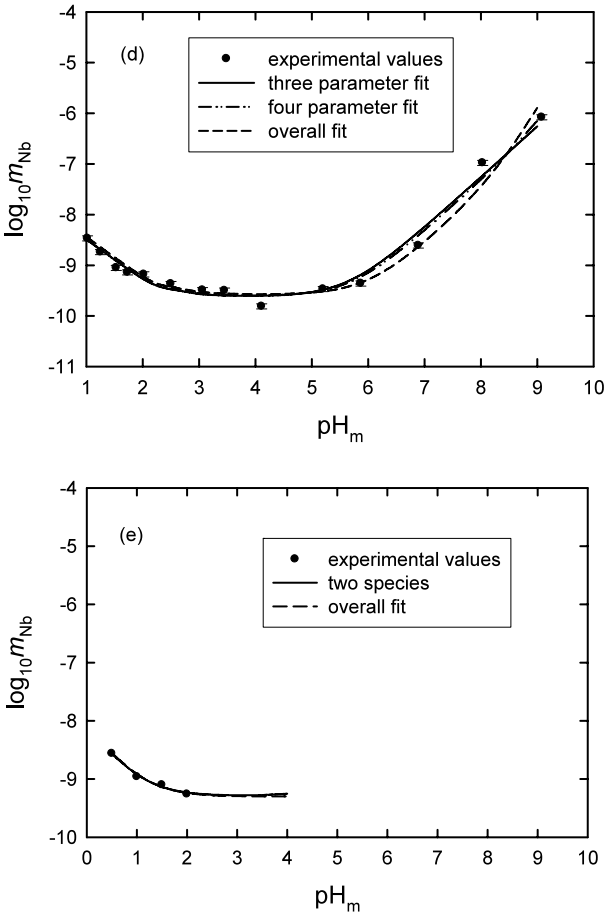

Fig. 3 (*Continued*)

existence of five mononuclear Nb(V) species[1] in solution, viz., $Nb(OH)_3^{2+}$, $Nb(OH)_4^{+}$, $Nb(OH)_5^{0}$, $Nb(OH)_6^{-}$ and $Nb(OH)_7^{2-}$ in equilibrium with B-Nb_2O_5, according to the generalized reaction:

$$0.5Nb_2O_5(cr) + 0.5(2n-5)H_2O(l) \rightleftarrows Nb(OH)_n^{5-n} + (n-5)H^+ \quad (7)$$

However, the trihydroxo species $Nb(OH)_3^{2+}$ could only be detected in the analysis of the 70 °C ($I_m = 1.0$ mol·kg^{-1}) data. The sudden appearance of this species at the highest temperature studied is counterintuitive, because hydrolysis of metal ions is known to increase

[1]The highest Nb(V) concentrations of ca. 10^{-5} mol·kg^{-1} were achieved at $pH_m \approx 9$, where the Etxebarria et al. [7] potentiometric investigation at $I_M = 3$ mol·L^{-1} (KCl) and 25 °C would suggest that the species $Nb_6O_{16}(OH)_3^{5-}$ might be dominant, at least when $m_{Nb} > 10^{-3}$ mol·kg^{-1}. Fits that included this species, instead of the $Nb(OH)_7^{2-}$ anion, gave sharply upturned solubility curves above $pH_m = 8.5$ that at 50 °C ($I_m = 1.0$ mol·kg^{-1}) yielded a $\log_{10} {}^*Q_s$ of ca. $-(51.0 \pm 0.3)$ for the reaction: $3Nb_2O_5(cr) + 4H_2O(l) \rightleftarrows Nb_6O_{16}(OH)_3^{5-} + 5H^+$. Such multinuclear species were not considered further in the work.

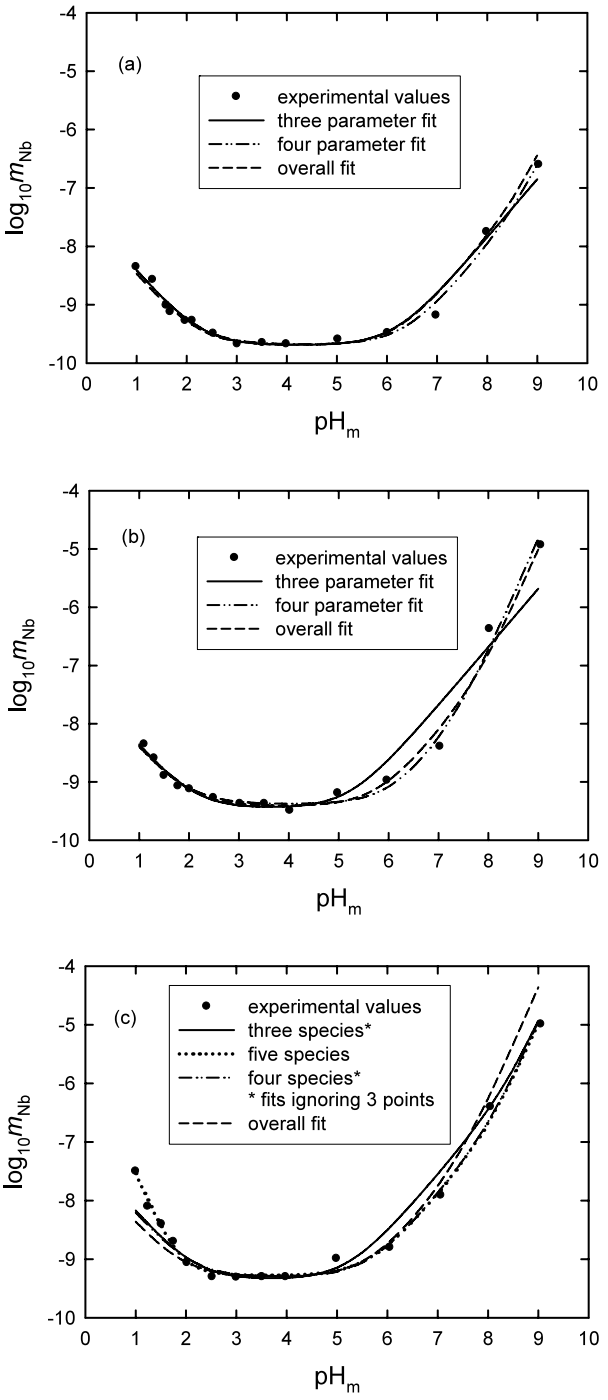

Fig. 4 Logarithm of the niobium(V) molality, $\log_{10} m_{\mathrm{Nb}}$, as a function of pH_m for an ionic strength of 1.0 mol·kg^{-1} at: 10.0 (**a**), 50.0 (**b**), and 70.0 °C (**c**)

Table 4 Solubility constants for B-Nb_2O_5 as functions of ionic strength and temperature (the results of alternative fits from excluding Q_{s7} are shown in italics)

t/°C	I_m[a]	$-\log_{10^*} Q_{s3}$	$-\log_{10^*} Q_{s4}$	$-\log_{10^*} Q_{s5}$	$-\log_{10^*} Q_{s6}$	$-\log_{10^*} Q_{s7}$	Fit factor
25.0	0.1		7.46 ± 0.35	9.20 ± 0.08	14.08 ± 0.05		2.081
25.0	0.3		*7.63 ± 0.20*	*9.21 ± 0.07*	*14.36 ± 0.07*		*2.353*
			7.64 ± 0.21	9.21 ± 0.07	14.39 ± 0.08	23.3 ± 0.2	2.407
25.0	0.5		*7.53 ± 0.15*	*9.51 ± 0.11*	*14.73 ± 0.09*		*3.484*
			7.53 ± 0.14	9.50 ± 0.10	14.82 ± 0.11	23.9 ± 0.4	3.245
25.0	1.0		*7.52 ± 0.09*	*9.62 ± 0.08*	*15.26 ± 0.09*		*3.104*
			7.53 ± 0.09	9.61 ± 0.08	15.33 ± 0.11	24.6 ± 0.4	3.094
25.0	6.0		8.16 ± 0.05	9.30 ± 0.04	–		0.839
10.0	1.0		*7.43 ± 0.08*	*9.70 ± 0.07*	*15.85 ± 0.09*		*2.885*
			7.44 ± 0.06	9.68 ± 0.06	16.03 ± 0.11	24.8 ± 0.2	2.375
50.0	1.0		*7.39 ± 0.21*	*9.45 ± 0.19*	*14.68 ± 0.18*		*6.837*
			7.42 ± 0.11	9.38 ± 0.08	15.40 ± 0.21	22.8 ± 0.1	3.294
70.0	1.0	*5.6 ± 0.1*	*7.78 ± 0.68*	*9.28 ± 0.07*	*14.93 ± 0.11*	*23.0 ± 0.1*	*2.498*
			7.24 ± 0.18	9.31 ± 0.08	14.92 ± 0.12	23.0 ± 0.1	2.964[b]
			7.20 ± 0.32	*9.35 ± 0.16*	*14.57 ± 0.14*		5.615[b]

[a]Units, mol·kg^{-1}

[b]Fit obtained by ignoring the three lowest pH values (see text)

with increasing temperature such that $Nb(OH)_3^{2+}$ should be destabilized with respect to $Nb(OH)_4^+$ and $Nb(OH)_5^0$ with increasing temperature. Therefore, the data taken at 70 °C at low pH_m were considered to be suspect and the three lowest pH_m values were excluded from the final fit, potentially leaving only four Nb(V) species to be considered. On the other hand, at the lowest ionic strength of 0.1 mol·kg^{-1} where hydrolysis is weakest, the fit of these solubility results did not converge with the inclusion of $Nb(OH)_7^{2-}$ so that only one entry is shown in Table 4 at this condition. For the remainder of the data, the existence of the three species, $Nb(OH)_4^+$, $Nb(OH)_5^0$ and $Nb(OH)_6^-$, is considered as being completely unambiguous. The question of the verifiable existence of the $Nb(OH)_7^{2-}$ species became a focus of the data reduction strategy. There are innumerable references to complexation studies of Nb(V) involving organic ligands where seven-fold coordination via a pentagonal bipyramidal structure have been assigned, e.g., [22–24]. Table 4 lists the $\log_{10} Q_{sn}$ values at each temperature and ionic strength providing (where possible) the results from weighted fits that either included or excluded (shown in italics) the $Nb(OH)_7^{2-}$ species, and the fit factor defined in Eq. 6.

The respective molal solubility quotients for the solubility reactions for the formation of $Nb(OH)_4^+$, $Nb(OH)_5^0$, $Nb(OH)_6^-$ and $Nb(OH)_7^{2-}$ according to the generalized equilibrium 7 are:

$$\log_{10} Q_{s4} = \log_{10}\left(m\{Nb(OH)_4^+\}/m\{H^+\}\right)$$
$$= \log_{10} K_{s4} - \log_{10}\left(\gamma\{Nb(OH)_4^+\}/\gamma\{H^+\}\right) + 1.5\log_{10}(a_w) \quad (8)$$

$$\log_{10} Q_{s5} = \log_{10}\left(m\{Nb(OH)_5^0\}\right)$$
$$= \log_{10} K_{s5} - \log_{10}\left(\gamma\{Nb(OH)_5^0\}\right) + 2.5\log_{10}(a_w) \quad (9)$$

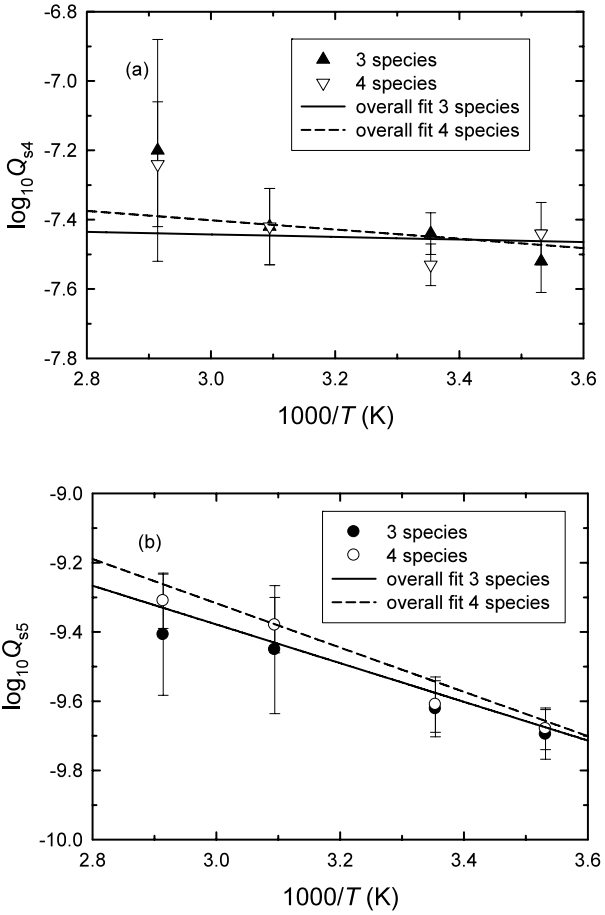

Fig. 5 Logarithm of the solubility quotients, $\log_{10} Q_{sn}$, as a function of reciprocal temperature in kelvin at an ionic strength of 1.0 mol·kg^{-1} for: $n = 4$ (**a**), $n = 5$ (**b**), $n = 6$ (**c**), and $n = 7$ (**d**)

$$\log_{10} Q_{s6} = \log_{10}\left(m\{\mathrm{Nb(OH)}_6^-\}m\{\mathrm{H}^+\}\right)$$
$$= \log_{10} K_{s6} - \log_{10}\left(\gamma\{\mathrm{Nb(OH)}_6^-\}\gamma\{\mathrm{H}^+\}\right) + 3.5\log_{10}(a_w) \quad (10)$$

$$\log_{10} Q_{s7} = \log_{10}\left(m\{\mathrm{Nb(OH)}_7^{2-}\}m\{\mathrm{H}^+\}^2\right)$$
$$= \log_{10} K_{s7} - \log_{10}\left(\gamma\{\mathrm{Nb(OH)}_7^{2-}\}\gamma\{\mathrm{H}^+\}^2\right) + 4.5\log_{10}(a_w) \quad (11)$$

Two approaches were taken to obtain a fit of the $\log_{10} Q_{sn}$ values at each ionic strength, i.e., to estimate the activity coefficient ratios. The first approach involved an empirical fit of these constants as combined functions of I_m and T including the appropriate Debye-Hückel terms, whereas the second approach was to apply the SIT equation for each data set at 25 °C only.

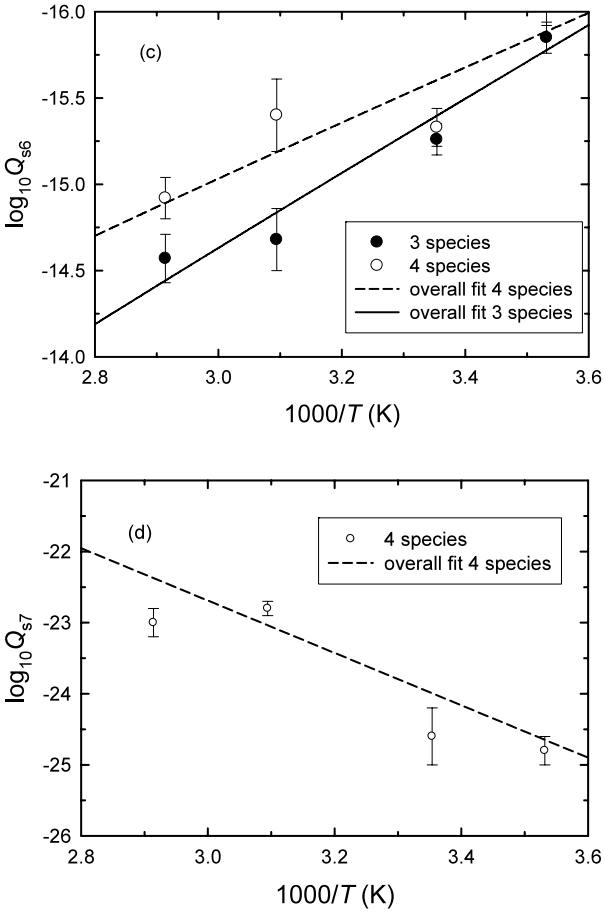

Fig. 5 (*Continued*)

The empirical approach involved the minimum number of adjustable parameters

$$\log_{10} Q_{sn} - \Delta z^2 D - 0.5(2n-5)\log_{10}(a_w) = a + b/T + cI_m + dI_m^2 \tag{12}$$

where $D = A(T)\sqrt{I_m}/(1 + 1.5\sqrt{I_m})$ which corresponds to the Debye-Hűckel term employed by the NEA [25], except that $A(T)$ is defined here as [26]:

$$A(T) = -2.97627 + 4.80688 \times 10^{-2}T - 2.6980 \times 10^{-4}T^2 + 7.49524 \times 10^{-7}T^3 - 1.02352 \times 10^{-9}T^4 \tag{13}$$

The differences between our choice and the NEA choice of $A(T)$ is $< 0.4\%$. Note that the fourth variable, d, was only employed for fitting of the $\log_{10} Q_{s4}$ data to $I_m = 6.0$ mol·kg^{-1}, but its inclusion did not have a significant effect on the calculated $\log_{10} K_{s4}$ values at infinite dilution. This approach has the advantage of fitting all of the available experimental results for each constant. Figures 5a–d and 6a–9a illustrate the effectiveness of

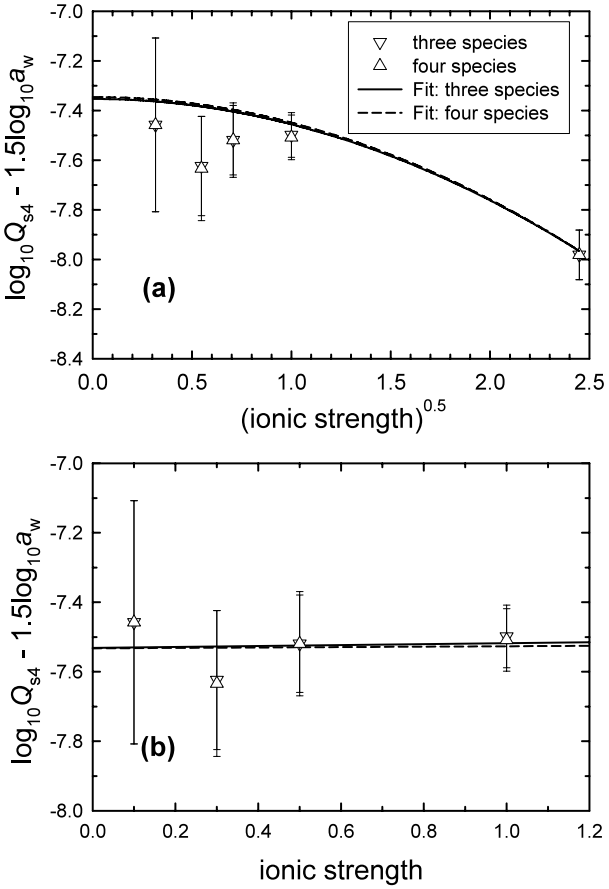

Fig. 6 Results of the application of the empirical fit of $\log_{10} Q_{s4}$ data as a function of the reciprocal temperature and ionic strength (shown as $\sqrt{I_m}$ for visual clarity); (**b**) application of the SIT equation to the $\log_{10} Q_{s4}$ data

Eq. 12 in representing all of the experimental data. The parameters in Eq. 13 and the infinite dilution $\log_{10} K_{sn}$ values are given in Table 5 according to the three-species' and four-species' fits. The corresponding thermodynamic quantities are discussed below.

Application of the SIT equation according to Eq. 14 was limited to the $\log_{10} Q_{s4}$ data at $I_m \leq 1.0$ mol·kg^{-1} and these plots are shown in Figs. 6b–9b, with the resulting $\log_{10} K_{sn}$ and $\Delta\varepsilon$ values given in Table 6:

$$\log_{10} Q_{sn} - \Delta z^2 D - 0.5(2n-5)\log_{10} a_w = \log_{10} K_{sn} - \Delta\varepsilon I_m \tag{14}$$

The $\log_{10} K_{sn}$ values from the restricted SIT data set are consistent with those obtained from the global fits within the combined 2σ estimated uncertainties. However, the estimated SIT interaction parameters have virtually no significance because of their large uncertainties, and values for $n = 5$–7 are obtained that are well outside the limits of accepted values for these charge types [25]. These values are only presented here to demonstrate that this approach was indeed tested and the linear regressions produced consistent $\log_{10} K_{sn}$ values. The ΔG° (298.15 K) values calculated from the respective global-fit $\log_{10} K_{sn}$ values for $n = 4$–7 in Table 5 are: (42.2 ± 0.5), (51.9 ± 0.2), (80.5 ± 0.7) and (136 ± 1) kJ·mol^{-1}. The corresponding ΔH° values obtained from the linear plots in Figs. 5a–d (b in Table 5),

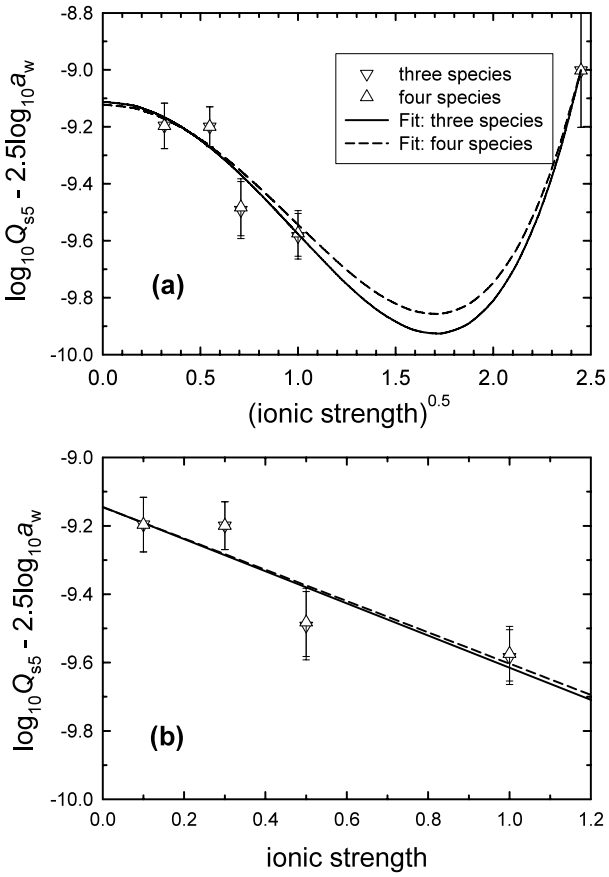

Fig. 7 (**a**) Results of the application of the empirical fit of $\log_{10} Q_{s5}$ as a function of the reciprocal temperature and ionic strength (shown as $\sqrt{I_m}$ for visual clarity); (**b**) application of the SIT equation to the $\log_{10} Q_{s5}$ data to $I_m = 1.0$ mol·kg^{-1}

which preclude a finite ΔC_p^o, are: (3 ± 4), (12 ± 2), (29 ± 8) and (66 ± 21) kJ·mol^{-1}. The resulting stepwise hydrolysis $\log_{10} K_{n,m}$ values at 25 °C are: $\log_{10} K_{4,5} = -(1.7 \pm 0.2)$, $\log_{10} K_{5,6} = -(5.0 \pm 0.3)$ and $\log_{10} K_{6,7} = -(9.8 \pm 0.7)$, with the accompanying enthalpy changes being: $\Delta H_{4,5}^o = (9 \pm 4)$, $\Delta H_{5,6}^o = (17 \pm 8)$ and $\Delta H_{6,7}^o = (37 \pm 22)$ kJ·mol^{-1}.

Wagman et al. [19] offered the following thermodynamic quantities for Nb_2O_5(cr), high temperature form, $\Delta_f G^o(298.15\ \text{K}, 0.1\ \text{MPa}) = -1766.0$ kJ·mol^{-1}, $\Delta_f H^o(298.15\ \text{K}, 0.1\ \text{MPa}) = -1899.5$ kJ·mol^{-1}, $S^o(298.15\ \text{K}, 0.1\ \text{MPa}) = 137.24$ J·K^{-1}·mol^{-1} and $C_p^o(298.15\ \text{K}, 0.1\ \text{MPa}) = 132.09$ J·K^{-1}·mol^{-1}, which together with their selected values for H_2O(l)$\{\Delta_f G^o(298.15\ \text{K}, 0.1\ \text{MPa}) = -237.129$ kJ·mol^{-1}, $\Delta_f H^o(298.15\ \text{K}, 0.1\ \text{MPa}) = -285.830$ kJ·mol^{-1}, $S^o(298.15\ \text{K}, 0.1\ \text{MPa}) = 69.91$ J·K^{-1}·mol^{-1} and $C_p^o(298.15\ \text{K}, 0.1\ \text{MPa}) = 75.291$ J·K^{-1}·mol$^{-1}\}$ yield the thermodynamic quantities for the aqueous Nb(V) species listed in Table 7.

All of the solubility data at $pH_m > 9$ show a discontinuity, probably favoring the transformation of Nb_2O_5 to a more insoluble solid phase, especially when one considers that the solution speciation must follow continuously from that at pH < 9 such that the $Nb(OH)_7^{2-}$ would immediately predominate because of its dependence on $m_{OH^-}^2$. The hexameric Nb(V) hydroxides described in Eqs. 3–5 should then appear as the niobate concentration further increases. The magnitude of the solubility discontinuity is illustrated in Fig. 10, where the curves result from the four-species model assuming that B-Nb_2O_5 is the solubility con-

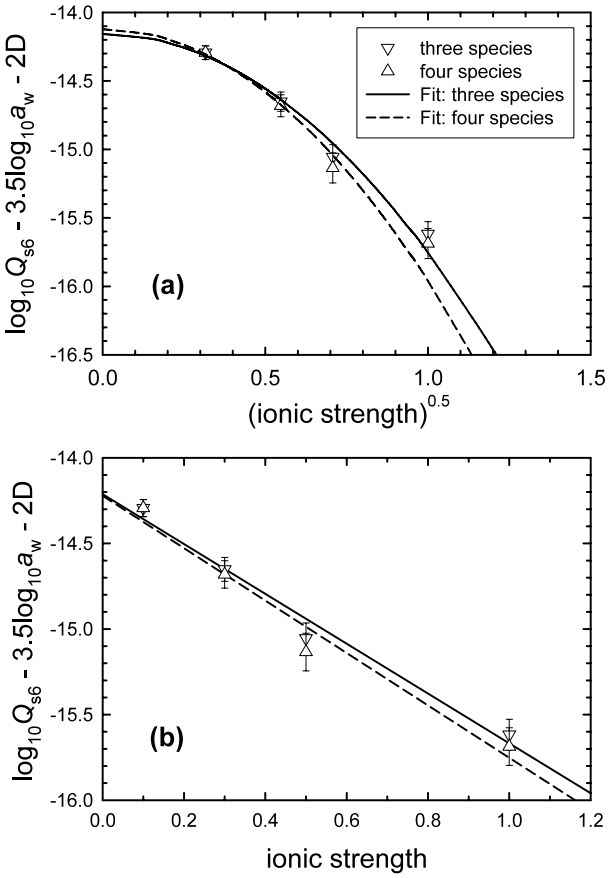

Fig. 8 (**a**) Results of the application of the empirical fit of the $\log_{10} Q_{s6}$ data as a function of reciprocal temperature and ionic strength (shown as $\sqrt{I_m}$ for visual clarity); (**b**) application of the SIT equation to the $\log_{10} Q_{s6}$ data to $I_m = 1.0$ mol·kg^{-1}

trolling solid phase. Not only is the trend in $\log_{10} m_{\mathrm{Nb}}$ much flatter but the dependence on ionic strength is lost within the scatter of the data. The suppressed solubility at $\mathrm{pH}_m > 9$ rules out the formation of colloidal material, but may indicate the formation of a mixed sodium niobate. In fact, XRD analyses of solids recovered after equilibration with acidic (10^{-2} mol·kg^{-1}, HNO_3) and basic (10^{-2} mol·kg^{-1}, NaOH) solutions at room temperature showed sharp peaks consistent only with crystalline B-Nb_2O_5 (see Table 1), thus indicating that any mixed oxide/hydroxide solid phase(s), which may have formed in the latter medium, is/are either present as a thin crystalline film on the B-Nb_2O_5 particles or as an thin amorphous layer.

4 Conclusions

Solubility measurements of well-characterized B-Nb_2O_5 as a function of temperature (10–70 °C), ionic strength (0.1–0.6 mol·kg^{-1}), and pH (1–9) have provided a unique thermodynamic platform for determination of the speciation and corresponding solubility constants. The fits of $\log_{10} m_{\mathrm{Nb}}$ versus pH_m incorporated mononuclear species from $Nb(OH)_4^+$ to $Nb(OH)_7^{2-}$. However, because only limited data points were obtainable for the latter

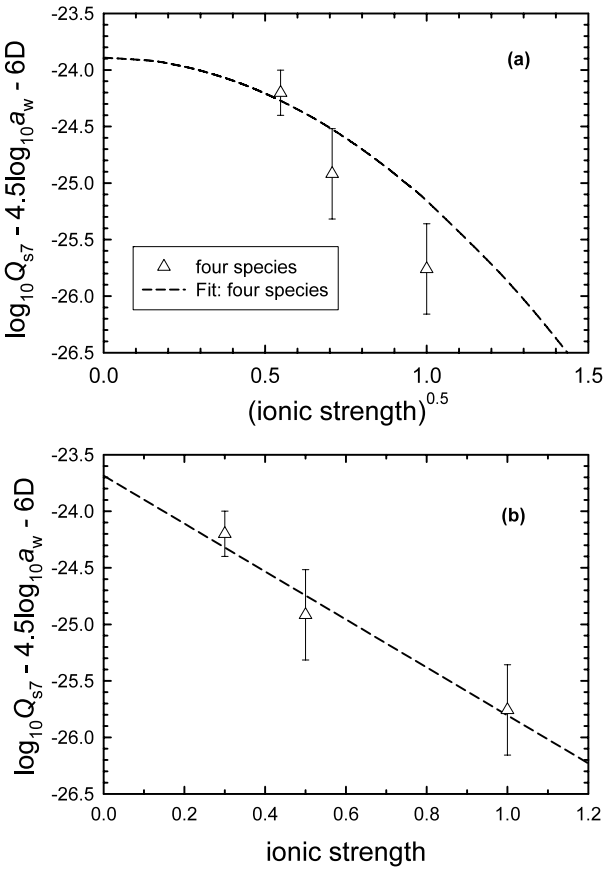

Fig. 9 (**a**) Results of the application of the empirical fit of the $\log_{10} Q_{s7}$ data as a function of reciprocal temperature and ionic strength (shown as $\sqrt{I_m}$ for visual clarity); (**b**) application of the SIT equation to the $\log_{10} Q_{s7}$ data to $I_m = 1.0$ mol·kg^{-1}

Table 5 Fitting parameters[a] for Eq. 12 and corresponding $\log_{10} K_{sn}$ (25.0 °C)[b] values with the alternative three-parameter (see Table 3) fit values shown in parentheses

Δz^2	N	a	b	c	$10^2 d$	$-\log_{10} K_{sn}$	R^2
−2	4	*−6.897 ± 0.725*	−133.9 ± 213.9	−0.103 ± 0.020	0	7.4 ± 0.2	0.840
		−7.23 ± 0.75	*−36.6 ± 221.2*	*−0.102 ± 0.018*	0	*7.4 ± 0.2*	*0.861*
0	5	−6.977 ± 0.445	−639.5 ± 130.4	−0.510 ± 0.086	−8.83 ± 1.42	9.1 ± 0.1	0.930
		−7.237 ± 0.711	*−559.0 ± 211.9*	*−0.561 ± 0.092*	*−9.65 ± 1.50*	*9.1 ± 0.2*	*0.929*
2	6	−8.992 ± 1.324	−1530. ± 392.	−1.837 ± 0.142	0	14.1 ± 0.3	0.977
		−7.175 ± 1.045	*−2082. ± 310*	*−1.597 ± 0.100*	0	*14.2 ± 0.3*	*0.986*
6	7	−12.312 ± 3.834	−3453. ± 1090.	−1.265 ± 0.832	0	23.9 ± 0.6	0.771

[a]The number of significant figures quoted is necessary to reproduce the calculated $\log_{10} Q_{sn}$ to better than ±0.01; with such a limited number of experimental values there is considerable covariance between these parameters, which are nevertheless considered to be the minimum number required

[b]Uncertainties are quoted at the 2σ level

Table 6 SIT Fitting parameters at 25.0 °C, providing $\log_{10} K_{sn}$ and their corresponding $\Delta\varepsilon$ values (kg·mol^{-1})[a], with the alternative three-parameter (see Table 3) values shown in parentheses, along with the resulting individual $\varepsilon(\mathrm{Nb(OH)}_n^{5-n}, \mathrm{ClO}_4^-)$ and $\varepsilon(\mathrm{Nb(OH)}_n^{5-n}, \mathrm{Na}^+)$ values (kg·mol^{-1})

Δz^2	N	$\log_{10} K_{sn}$	$\Delta\varepsilon$	$\varepsilon(\mathrm{Nb(OH)}_n^{5-n}, \mathrm{ClO}_4^-)$[b]	$\varepsilon(\mathrm{Nb(OH)}_n^{5-n}, \mathrm{Na}^+)$[b]
−2	4	-7.57 ± 0.14	0.1 ± 0.2	0.1 ± 0.2	
		−7.58 ± 0.13	*0.1 ± 0.2*		
0	5	*−9.13 ± 0.15*	*−0.5 ± 0.3*	*−0.5 ± 0.3*	-0.5 ± 0.3
		-9.13 ± 0.16	-0.5 ± 0.3		
2	6	-14.16 ± 0.14	-1.6 ± 0.3		-1.6 ± 0.3
		−14.17 ± 0.12	-1.5 ± 0.3		
6	7	-23.6 ± 0.4	-2.3 ± 0.8		-2.7 ± 0.8

[a]Uncertainties are quoted at the 2σ level

[b]$\varepsilon(\mathrm{H}^+, \mathrm{ClO}_4^-) = (0.14 \pm 0.02)$ kg·mol^{-1} [25]

Table 7 Thermodynamic quantities for the aqueous niobium(V) species based on the "four-species" model

	$\mathrm{Nb(OH)}_4^+$	$\mathrm{Nb(OH)}_5^0$	$\mathrm{Nb(OH)}_6^-$	$\mathrm{Nb(OH)}_7^{2-}$
$\Delta_f G^o$(298.15 K, 0.1 MPa) kJ·mol^{-1}	-1196 ± 8	-1424 ± 8	-1632 ± 8	-1814 ± 8
$\Delta_f H^o$(298.15 K, 0.1 MPa) kJ·mol^{-1}	-1376 ± 9	-1652 ± 8	-1921 ± 11	-2170 ± 22
S^o(298.15 K, 0.1 MPa) J·K^{-1}·mol^{-1}	40 ± 12	110 ± 11	142 ± 14	147 ± 23
C_p^o(298.15 K, 0.1 MPa)[a] J·K^{-1}·mol^{-1}	179	254	330	405

[a]These values are approximate, based on the assumption that $\Delta C_p^o = 0$ J·K^{-1}·mol^{-1} for each solubility reaction, given the experimental uncertainties and the narrow temperature range investigated

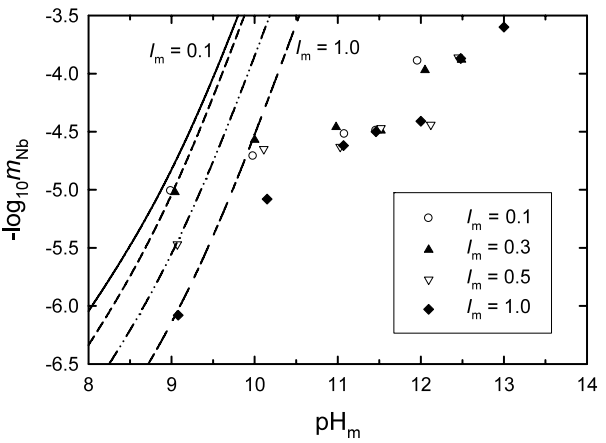

Fig. 10 Logarithm of the niobium(V) molality, $\log_{10} m_{\mathrm{Nb}}$, as a function of pH_m (>9) at 25 °C for various ionic strengths: 0.1, 0.3, 0.5, and 1.0 mol·kg^{-1} compared with the predicted curves for the "four-species" model where only B-N_2O_5(cr) would control the observed solubility

species, alternative fits are offered which excluded this species. Thermodynamic quantities are provided based on the measurements at four temperatures over a range of 60 °C. No reasonable interaction parameters could be extracted from applications of the SIT.

Acknowledgements The financial support was provided by ANDRA (Agence Nationale pour la gestion des Déchets RAdioactifs), France, under contracts C RP 0. CRE 95.001 (05 006 AA0), C RP 0. CRE 96.002 (GT 005 AA0), and C RP 0. CRE 97.003 (316 454 A0).

References

1. Cotton, F.A., Wilkinson, G.: Advanced Inorganic Chemistry, 2nd edn. Wiley-Interscience, New York (1988), p. 787
2. Hofmann, A.W.: Mantle geochemistry: the message from oceanic volcanism. Nature **385**, 219–229 (1997)
3. Reimann, C., de Caritat, P.: Chemical Elements in the Environment—Factsheets for the Geochemist and Environmental Scientist. Springer, Berlin (1998), p. 398
4. Pudjanto, B.A.: The chemical state of fission products in uranium-oxide fuel. In: Prosiding Seminar Nasional Sainsdan Teknik Nukir P3TkN-BATAN, Bandung, Indonesia, 14–15 June 2005, pp. 236–244
5. Babko, A.K., Lukachina, V.V., Nabivanets, B.I.: Solubility and acid-base properties of tantalum and niobium hydroxides. Russ. J. Inorg. Chem. **8**, 957–961 (1963)
6. Baes, C.F. Jr., Mesmer, R.E.: The Hydrolysis of Cations. Wiley-Interscience, New York (1976)
7. Etxebarria, N.E., Fernández, L.A., Madariaga, J.M.: On the hydrolysis of niobium(V) and tantalum(V) in 3 mol·dm^{-3} KCl at 25 °C. Part 1. Construction of a thermodynamic model for Nb^{V}. J. Chem. Soc., Dalton Trans. 3055–3059 (1994)
8. Mesmer, R.E., Holmes, H.F.: pH definition and measurement at high temperatures and pressures. J. Solution Chem. **21**, 725–744 (1992)
9. Spinner, B.: Étude quantitative de l'hydrolyse des niobates de potassium. Rev. Chim. Min. **5**, 839–868 (1968)
10. Goiffon, A., Granger, R., Bockel, C., Spinner, B.: Étude des équilibres dans les solutions alcalines du niobium V. Rev. Chim. Min. **10**, 487–502 (1973)
11. Goiffon, A., Spinner, B.: Spectres Raman des solutions aqueuses du niobates de potassium. Rev. Chim. Min. **11**, 262–268 (1974)
12. Jander, G., Ertel, D.: Über Niobsäuren und Wasserlösliche Alkaliniobate. I Lichtabsorptions- und Diffusionsmessungen an Alkaliniobatlösungen. J. Inorg. Nucl. Chem. **14**, 71–76 (1960)
13. Neumann, G.: On the hydrolysis of niobates in 3 *M* K(Cl) medium. Acta Chem. Scand. **18**, 278–280 (1964)
14. Jander, G., Ertel, D.: Über Niobsäuren und Wasserlösliche Alkaliniobate. II Präparitiv-analytische Untersuchungen. J. Inorg. Nucl. Chem. **14**, 77–84 (1960)
15. Jander, G., Ertel, D.: Über Niobsäuren und Wasserlösliche Alkaliniobate. III Kinduktometrische Titrationen und vergleichende Röntgengraphische Untersuchungen. Das Hydrolyseschema der Isopolyniobate. J. Inorg. Nucl. Chem. **14**, 85–90 (1960)
16. Wesolowski, D.J., Ziemniak, S.E., Anovitz, L.M., Machesky, M.L., Bénézeth, P., Palmer, D.A.: Solubility and surface adsorption characteristics of metal oxides. In: Palmer, D.A., Fernández-Prini, R., Harvey, A.H. (eds.) Aqueous Systems at Elevated Temperatures and Pressures: Physical Chemistry in Water, Steam and Hydrothermal Solutions, vol. 14, pp. 493–595. Elsevier/Academic Press, Amsterdam (2004)
17. Guillaumont, R., Franck, J.C., Muxart, R.: Contribution à l'étude de l'hydrolyse du niobium. Radiochem. Radioanal. Lett. **4**, 73–79 (1970)
18. Lindqvist, I.: The structure of the hexaniobate ion in $7Na_2O{\cdot}6Nb_2O_5{\cdot}32H_2O$. Ark. Kemi **5**, 247–250 (1953)
19. Wagman, D.D., Evans, W.H., Parker, V.B., Schumm, R.H., Halow, I., Bailey, S.M., Churney, K.L., Nuttall, R.L.: The NBS tables of chemical thermodynamic properties. J. Phys. Chem. Ref. Data **11**, 2–207 (1982)
20. Anderegg, G., Rao, L., Puigdomenech, I., Tochiyama, O.: In: Mompean, J., Illemassène, M. (eds.) Chemical Thermodynamics of Compounds and Complexes of U, Np, Pu, Am, Tc, Se, Ni and Zr with Selected Organic Ligands. Elsevier, Amsterdam (2005)
21. Robinson, R.A., Stokes, R.H.: Electrolyte Solutions, 2nd edn. Butterworths, London (1959)

22. Serafím, M.J.S., Bessler, K.E., Lemos, S.S., Sales, M.J.A., Ellena, J.: The preparation of new oxoniobium(V) complexes from hydrated niobium(V) oxide: the crystal and molecular structure of oxotris(2-pyridinolato-*N*-oxide)niobium(V). Trans. Met. Chem. **32**, 112–116 (2007)
23. Gudasi, K., Maravalli, P., Goudar, T.: Thermokinetic and spectral studies of niobium(V) complexes with 3-substituted-4-amino-5-mercapto-1,2,4-triazole Schiff bases. J. Serb. Chem. Soc. **70**, 643–650 (2005)
24. Vachirapatama, N., Macka, M., Paull, B., Műnker, C., Haddad, P.R.: Determination of niobium(V) and tantalum(V) as 4-(2-pyridylazo)resorcinol–citrate ternary complexes in geological materials by ion-interaction reversed-phase high-performance liquid chromatography. J. Chrom. A **850**, 257–268 (1999)
25. Grenthe, I., Puigdomenech, I. (eds.): Modeling in Aquatic Chemistry. OECD, Paris (1997)
26. Mesmer, R.E., Baes, J.F. Jr.: Phosphoric acid dissociation equilibria in aqueous solutions to 300 °C. J. Solution Chem. **3**, 307–322 (1974)